Dipole-exchange spin-wave modes in very-thin-film antiferromagnets

R. L. Stamps and R. E. Camley

Department of Physics, University of Colorado at Colorado Springs, P.O. Box 7150, Colorado Springs, Colorado 80907-7150
(Received 11 March 1986; revised manuscript received 18 September 1986)

We study spin-wave modes in very-thin-film antiferromagnets in the wavelength region where both exchange and dipolar energies are important. Exchange boundary conditions appropriate to the (100) and (110) surfaces of a bcc crystal are derived and solved consistently with the equations of motion to yield the dispersions for spin-wave modes in various thin-film geometries. The effects of surface conditions are explored, illustrating the importance of free and pinned surface spins and also revealing a dramatic dependence on microscopic film surface geometry. In calculations for MnF$_2$ we show how the dipole-exchange modes can be localized to one surface in certain film geometries *without* the presence of an applied field.

I. INTRODUCTION

Many of the unique features (nonreciprocal surface waves, backward traveling volume waves, etc.) of ferromagnetic spin waves have found application in practical devices such as the delay lines and filters which are used in microwave processing technologies.[1,2] In these devices it is the dipolar fields which play an important role. Antiferromagnetic spin waves where dipolar interactions are important, however, have not received as much attention.[3-6] Nonetheless, in a recent experiment nonreciprocal reflection of infrared radiation was observed from the surface of antiferromagnetic MnF$_2$.[7] The nonreciprocal reflection can be attributed to the influence of dipolar fields.

Previous treatments of dipole-influenced spin waves in bounded antiferromagnets have concentrated on the long-wavelength region. In this paper we consider the dipole-exchange modes of an antiferromagnetic film which is thin enough that the long-wavelength approximation is not sufficient. An advantage of this treatment is that the dependence of spin waves on surface conditions may be investigated. For example, in ferromagnets, it is well known that surface anisotropy fields may lead to the pinning of surface spins.[8] Experimental magnetic resonance[9,10] and light-scattering studies[11-13] yield spectra with line intensities and positions that significantly depend on spin pinning at the surface. A great deal of information about surface conditions may thus be obtained from spin-wave experiments on magnetic crystals.

Surface anisotropy and exchange fields affect modes in antiferromagnets as well. Due to the reduced number of neighbors at the surface, the exchange field that a surface spin experiences may be greatly reduced compared to the exchange field felt by a spin in the bulk of the material. As we will see, this may also lead to spin pinning at the surface of an antiferromagnet. This is in stark contrast to the results for ferromagnets where the reduction in the number of neighbors at the surface does *not* lead to any pinning effects.

The microscopic structure is also important for antiferromagnets, especially for thin films. For example, the (110) surface of a body-centered cubic antiferromagnet

contains spins from both magnetic sublattices while a (100) surface contains spins from only one sublattice. As we shall see, spin waves propagating in a structure where the surface contains both magnetic sublattices have different properties from those propagating in a film where the surface contains only one magnetic sublattice, and antiferromagnetic resonance experiments should be very sensitive to these differences. With this sensitivity to surface construction, an examination of spin-waves modes in very thin films is necessary to help characterize the quality of antiferromagnetic films which are presently being grown.[14]

We will want to compare our results for the dipole-exchange spin-wave modes in thin antiferromagnetic films to earlier results in thicker films.[3] We consider a geometry where the easy axis of the antiferromagnet lies along the z axis and the y axis is normal to the surfaces of the film. This geometry is illustrated in Fig. 1. For spin waves propagating parallel to the surface but perpendicular to the easy axis in very thick films, there are three important frequencies:

$$\omega_1 = \gamma[H_a(2H_{ex} + H_a)]^{1/2} , \tag{1}$$

$$\omega_s = \gamma[H_a(2H_{ex} + H_a + 4\pi M)]^{1/2} , \tag{2}$$

$$\omega_2 = \gamma[H_a(2H_{ex} + H_a + 8\pi M)]^{1/2} , \tag{3}$$

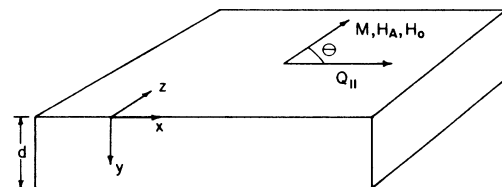where H_a is the anisotropy field, H_{ex} is the mean ex-

FIG. 1. Film geometry. The film is aligned with the sublattice magnetizations parallel and antiparallel to the z axis. The surfaces are parallel to the xz plane and are at $y = +d/2$ and $y = -d/2$. An applied field may lie in the $+z$ direction. The spin-wave vector, $Q_{||}$, makes an angle θ with the z axis.

change field, and M is the saturation magnetization of a sublattice. These results hold only in the long-wavelength limit. ω_1 and ω_2 are the frequencies of bulk spin waves. There is an infinite number of degenerate spin wave at each of these frequencies corresponding essentially to an infinite set of standing waves in the y direction with different wavelengths. We note that ω_1 is the well-known antiferromagnetic resonance frequency. In addition to the bulk modes, there are two degenerate surface modes with frequency ω_s which exist between the two bulk bands. The two modes correspond to waves which have odd and even symmetry about the midplane of the film. For thin films, this degeneracy is removed with the even mode having a lower frequency.

When a field is applied, the above formulas do not hold. The upper bulk modes are shifted up in frequency, and the lower bulk modes are shifted down, but the degeneracy is not removed. The degeneracy of the surface modes, however, is removed, and one mode is shifted upward and the other downward, and an interesting localization occurs. The upward shifted wave propagating along the positive x axis is localized at the lower surface of the film while the wave propagating along the negative x axis is localized at the upper surface. The surface modes which are shifted lower also display localization, but the localization is reversed. The bulk modes also show some slight localization. Even weak applied fields of only a few hundred gauss can strongly localize the surface modes.

In this paper we are concerned with spin-wave modes in very thin antiferromagnetic films. Such films necessarily have short wavelengths due to the standing-wave character of the spin waves inside the film. Spin waves with shorter wavelengths but that include dipolar fields have been studied by Louden and Pincus[15] for an infinite antiferromagnet. Their results show that the higher-order terms in the expansion of the magnetization add effective fields which are proportional to the square of the wave vector. We have found that these additional exchange terms lift the degeneracy of the bulk modes in thin films and shift the modes upwards in frequency. This holds for both the upper and lower bulk bands.

The surface spin waves are not shifted strongly by the addition of higher-order exchange terms. This is easily understood. The magnitude of the decay constant determining the penetration depth of the surface mode has, even for thin films, approximately the same magnitude as the wave-vector component parallel to the surface of the films. The surface modes thus retain nearly the same profile for different thicknesses and hence nearly the same frequency. The results is that the lower bulk band moves upward through the surface modes as the thickness is reduced. There is some interaction between bulk and surface modes even though the surface modes are predominantly dipolar in character and the lower bulk modes are largely governed by exchange fields. We note that a similar behavior occurs in ferromagnets.[6]

In Sec. II, we will present the theoretical development necessary for the treatment of spin waves in thin antiferromagnetic films. This includes the derivation of boundary conditions for the various surfaces and the development of a method to find the dispersion relation for spin-wave modes propagating at an arbitrary direction, parallel to the surface of the film. In Sec. III we present numerical results for the dispersion curves and for the spatial variation of the fluctuating portion of the magnetizations and the magnetic scalar potential.

II. THEORY

The geometry of the film is shown in Fig. 1. The surfaces of the film are parallel to the xz plane and the film has thickness d. We consider a simple two-sublattice model where the magnetizations in one sublattice are taken parallel to the z axis and those in the other sublattice are antiparallel to the z axis. The applied field $\mathbf{H}_0$ is in the positive z direction. The wave vector $\mathbf{Q}_{\parallel}$ makes an angle θ with the z axis and lies in a plane parallel to the surfaces.

The dipole-exchange waves must satisfy both Bloch's equations of motion and the magnetostatic form of Maxwell's equations. For our two-sublattice model, these read

$$d\mathbf{M}^A/dt = \gamma \mathbf{M}^A \times \mathbf{H}^A ,$$ (4)

$$d\mathbf{M}^B/dt = \gamma \mathbf{M}^B \times \mathbf{H}^B ,$$ (5)

where γ is the gyromagnetic ratio and $\mathbf{H}^A$ and $\mathbf{H}^B$ are the effective fields acting on sublattice A and B, respectively. We have

$$\mathbf{H}^A = \mathbf{z}(H_0 + H_a) + \mathbf{H}_{ex}^A + \mathbf{h}_d ,$$ (6)

$$\mathbf{H}^B = \mathbf{z}(H_0 - H_a) + \mathbf{H}_{ex}^B + \mathbf{h}_d .$$ (7)

$\mathbf{H}_0$ is the applied field in the z direction, and $\mathbf{H}_a$ is the anisotropy field directing the magnetizations along the z axis. $\mathbf{h}_d$ is the magnetostatic field that satisfies $\nabla \times \mathbf{h}_d = 0$ and is given by $\mathbf{h}_d = -\nabla \phi$. $\mathbf{H}_{ex}^A$ and $\mathbf{H}_{ex}^B$ are the effective fields acting on the A and B sublattices. The effective exchange field at position x due to sublattice A is given by

$$\mathbf{H}_{ex}^B = \lambda \sum \mathbf{M}^A(\mathbf{x} + \delta) .$$ (8)

The exchange constant is λ and the sum is over the nearest neighbors only. In a continuum limit, we want all our variables to be evaluated at the same point. We thus expand $\mathbf{M}^A(\mathbf{x} + \delta)$ about $\mathbf{x}$

$$\mathbf{M}^A(\mathbf{x} + \delta) = \mathbf{M}^A(\mathbf{x}) + (\delta \cdot \nabla)\mathbf{M}^A(x)$$
$$+ (\delta \cdot \nabla)^2 \mathbf{M}^A(\mathbf{x}) + \cdots .$$ (9)

For exchange fields in the bulk, this expansion leads to the expressions

$$\mathbf{H}_{ex}^B(\mathbf{x}) = \lambda(8 + a^2\nabla^2)\mathbf{M}^A(\mathbf{x})$$ (10)

and

$$\mathbf{H}_{ex}^A(\mathbf{x}) = \lambda(8 + a^2\nabla^2)\mathbf{M}^B(\mathbf{x}) ,$$ (11)

where a is the lattice constant of the material.

The first-order terms and second-order cross terms vanish in the sum over nearest neighbors because of the symmetry of the cubic lattice. This is not true at a surface and will in fact lead to a set of boundary conditions for the magnetizations.

Substitution of these fields into Bloch's equations and linearizing results in four equations. A fifth is found from the condition that $\nabla \cdot \mathbf{B} = 0$ which yields

$$-\nabla^2 \phi + 4\pi \nabla \cdot (\mathbf{M}^A + \mathbf{M}^B) = 0 . \tag{12}$$

In order to solve these five equations, we assume that all variables $(M_x^A, M_y^A, M_x^B, M_y^B, \phi)$ have the following behavior:

$$\exp[i(\mathbf{Q}_{||} \cdot \mathbf{x}_{||} - \omega t) + \alpha y] .$$

The position vector $\mathbf{x}_{||}$ is defined as $\mathbf{x}_{||} = \mathbf{x}x + \mathbf{z}z$ and the wave vector parallel to the surface is $\mathbf{Q}_{||} = \mathbf{x}Q_x + \mathbf{z}Q_z$. The

superscripts on M refer to the sublattice and the subscripts mark the spatial components. This represents an excitation which is plane-wave-like parallel to the surfaces of the film. For the direction perpendicular to the film, the y direction, the excitation may have exponentially increasing or decreasing character (α is real and positive or negative) or may have a sinusoidal character (α is imaginary). The first case indicates a surface wave, while the second case is a bulk wave.

With these assumptions, Eqs. (4), (5), and (12) can be written in the following matrix form:

$$\begin{bmatrix} -i\omega/\gamma & -H_+ & 0 & D & \alpha M \\ H_+ & -i\omega/\gamma & -D & 0 & iQ_x M \\ 0 & -D & -i\omega/\gamma & -H_- & -\alpha M \\ D & 0 & H_- & -i\omega/\gamma & -iQ_x M \\ 4\pi iQ_x & -4\pi\alpha & 4\pi iQ_x & -4\pi\alpha & Q^2 - \alpha^2 \end{bmatrix} \begin{bmatrix} M_x^A \\ M_y^A \\ M_x^B \\ M_y^B \\ \phi \end{bmatrix} = \begin{bmatrix} 0 \\ 0 \\ 0 \\ 0 \\ 0 \end{bmatrix} . \tag{13}$$

Here we have defined

$$M = M_z^A = -M_z^B , \tag{14}$$

$$H_e = -8\lambda M , \tag{15}$$

$$H_\pm = H_0 \pm (H_a + H_e) , \tag{16}$$

$$D = -H_e[1 + a^2(\alpha^2 - Q_{||}^2)/8] . \tag{17}$$

For Eq. (13) to hold, the determinant of the matrix must be zero. This condition gives us a relation between α, ω, and $Q_{||}$. Considered as a function of α, the determinant of this matrix is a fifth-order polynomial in α^2. An explicit expression for α is

$$(\alpha^2 - Q_{||}^2)[\omega^2(H_+ - H_-)/\gamma^2 + D^2(H_+ - H_-) + H_+ H_-(H_+ - H_- + 2D) + 2D^3]$$
$$+ (\alpha^2 - Q_{||}^2)[-\omega^4/\gamma^4 + \omega^2(H_+^2 + H_-^2 - 2D^2)/\gamma^2 - H_+ H_-(2D^2 + H_+ H_-) - D^4] = 0 . \tag{18}$$

We will later require an expression containing only the first six orders in α. This is obtained by replacing D^3 and D^4 in Eq. (18) by

$$D^3 = -[1 + 3(\alpha^3 - Q_{||}^2) + 3(\alpha^2 - Q_{||}^2)^2]H_e^3 , \tag{19}$$

$$D^4 = [1 + \tfrac{1}{2}(\alpha^2 - Q_{||}^2) + \tfrac{3}{32}(\alpha^2 - Q_{||}^2)^2]H_e^4 . \tag{20}$$

The resulting expression is consistent with the dispersion relation given in Ref. 15.

We expect our solution for the thin-film problem to be a superposition of ten waves, each with a different characteristic α. Thus we may write the magnetizations and potential as sums:

$$M_x^A = \sum_j A_x^j \exp[i(\mathbf{Q}_{||} \cdot \mathbf{x}_{||} - \omega t) + \alpha_j y] , \tag{21}$$

$$M_y^A = \sum_j A_y^j \exp[i(\mathbf{Q}_{||} \cdot \mathbf{x}_{||} - \omega t) + \alpha_j y] , \tag{22}$$

$$M_x^B = \sum_j B_x^j \exp[i(\mathbf{Q}_{||} \cdot \mathbf{x}_{||} - \omega t) + \alpha_j y] , \tag{23}$$

$$M_y^B = \sum_j B_y^j \exp[i(\mathbf{Q}_{||} \cdot \mathbf{x}_{||} - \omega t) + \alpha_j y] , \tag{24}$$

$$\phi = \sum_j \phi^j \exp[i(\mathbf{Q}_{||} \cdot \mathbf{x}_{||} - \omega t) + \alpha_j y] . \tag{25}$$

Since some of the α will be real and some will be imaginary, we see that every mode has both surfacelike and bulklike characteristics.

Through the use of the equation of motion matrix, we can relate A_y^j, B_x^j, B_y^j, and ϕ^j to A_x^j for each individual ω, $\mathbf{Q}_{||}$, and α_j. The result is that we have ten unknowns, $A_x^1 - A_x^{10}$. These ten unknowns are then found from the boundary conditions.

A. Boundary conditions

The dipole-exchange modes must satisfy both the electromagnetic Maxwell boundary conditions plus conditions imposed by the inclusion of exchange interactions. A general expression for boundary conditions that account for exchange interactions can be derived in the usual manner of integrating the equations of motion over a small volume that includes the boundary.[8] The resulting expression is a linear combination of the components and normal derivatives of the components of the magnetizations.

In this paper we refer to the latter as the "free-spin" terms and the former are the "pinned-spin" terms.

We use a somewhat different method[17] which yields the same results. The basic idea is that an eigenmode of the system must have all spins oscillating at the same frequency. In particular, this requires the frequency of a surface spin to be the same as that of a bulk spin. Thus the torques (and equations of motion) on a surface spin must be the same as that of the bulk spin. Normally, the surface spins see a different field than the bulk spins because they have fewer nearest neighbors. We can require that the surface spins have the same equations of motion as the bulk spins and thereby obtain a boundary condition. The equations of motion for a surface spin are

$$\frac{d\mathbf{M}_{\text{surf}}}{dt} = \gamma(\mathbf{M}_{\text{surf}} \times \mathbf{H}_{\text{surf}}) , \tag{26}$$

where $\mathbf{H}_{\text{surf}}$ is the effective field acting on the surface spin. We now add and subtract $\mathbf{H}_{\text{bulk}}$ to obtain

$$\frac{d\mathbf{M}_{\text{surf}}}{dt} = \gamma(\mathbf{M}_{\text{surf}} \times \mathbf{H}_{\text{bulk}}) + \gamma\mathbf{M}_{\text{surf}} \times (\mathbf{H}_{\text{surf}} - \mathbf{H}_{\text{bulk}}) . \tag{27}$$

Equation (27) reduces to the bulk equations of motion if

$$\gamma\mathbf{M}_{\text{surf}} \times (\mathbf{H}_{\text{surf}} - \mathbf{H}_{\text{bulk}}) = 0 . \tag{28}$$

We see that the above equation is an effective boundary condition. The particular form of boundary conditions depends on the particular surface under consideration.

B. (110) surface

We have a total of five equations per boundary: one from the magnetostatic boundary conditions, two from the equations of motion for the A sublattice, and two from the equations of motion for the B sublattice. As an example, we explicitly derive the boundary conditions for the A sublattice spins. When one expands the magnetizations about the position of the spin of interest, one obtains the effective exchange field acting at the surface:

$$\left[6 - a\sqrt{2}\frac{\partial}{\partial y} + a^2\frac{\partial^2}{\partial x^2} + \frac{a^2}{2}\frac{\partial^2}{\partial y^2} + \frac{3}{4}a^2\frac{\partial^2}{\partial z^2} \right]\lambda\mathbf{M}^B . \tag{29}$$

In addition, due to surface conditions (roughness, contamination, the lowering of the number of nearest neighbors, etc.) the anisotropy field at the surface may also be different. The boundary condition Eq. (28) at the upper surface becomes

$$[-2H_e + 8(\Delta H_a)_z]M_y^B - H_e\left[2 + a\sqrt{2}\frac{\partial}{\partial y} + a^2\left[\frac{1}{2}\frac{\partial^2}{\partial y^2} + \frac{1}{4}\frac{\partial^2}{\partial z^2}\right]\right]M_y^A + 8(\Delta H_a)_y M = 0 , \tag{30}$$

$$[2H_e - 8(\Delta H_a)_z]M_x^B + H_e\left[2 + a\sqrt{2}\frac{\partial}{\partial y} + a^2\left[\frac{1}{2}\frac{\partial^2}{\partial y^2} + \frac{1}{4}\frac{\partial^2}{\partial z^2}\right]\right]M_x^A - 8(\Delta H_a)_x M = 0 , \tag{31}$$

where ΔH_a is the difference in the anisotropy fields between the bulk and surface spins. Note that the boundary condition above contains both free-spin terms $(\partial M/\partial y)$ as well as pinned-spin terms (M) even if there is no change in the anisotropy fields. This is in contrast to the result in the ferromagnet where spin pinning comes primarily from surface anisotropy fields.

In the limit that $\Delta H_A = 0$, these two equations reduce to a particularly simple form:

$$2M_y^B + \left[2 + a\sqrt{2}\frac{\partial}{\partial y} + a^2\left[\frac{1}{2}\frac{\partial^2}{\partial y^2} + \frac{1}{4}\frac{\partial^2}{\partial z^2}\right]\right]M_y^A = 0 , \tag{32}$$

$$2M_x^B + \left[2 + a\sqrt{2}\frac{\partial}{\partial y} + a^2\left[\frac{1}{2}\frac{\partial^2}{\partial y^2} + \frac{1}{4}\frac{\partial^2}{\partial z^2}\right]\right]M_x^A = 0 . \tag{33}$$

A quick estimate shows that the pinning terms often dominate in magnitude over the free-spin terms in the long-wavelength limit. An important exception to this occurs when $M_x^A = M_x^B$. In this case, the pinning-like terms cancel and the free-spin term is dominant. We note that this case *does* occur. In the long-wavelength limit, for example, when $Q_x/Q_y \gg 1$, then $M_x^A = M_x^B$ for the lower modes and $M_y^A = M_y^B$ for the upper modes. When $Q_x/Q_y \ll 1$, the y components are equal and opposite for the lower modes and the x components are equal for the upper modes.[18] Such dynamic pinning, in cases where the degree of pinning depends strongly on the wave properties itself, has been discussed previously for ferromagnets.[19,20]

The remaining boundary conditions may be derived in a similar manner. We obtain

$$[-2H_e + 8(\Delta H_a)_z]M_y^A + H_e\left[2 + a\sqrt{2}\frac{\partial}{\partial y} + a^2\left[\frac{1}{2}\frac{\partial^2}{\partial y^2} + \frac{1}{4}\frac{\partial^2}{\partial z^2}\right]\right]M_y^B - 8(\Delta H_a)_y M = 0 , \tag{34}$$

$$[-2H_e - 8(\Delta H_a)_z]M_x^A - H_e \left[2 + a\sqrt{2}\frac{\partial}{\partial y} + a^2 \left[\frac{1}{2}\frac{\partial^2}{\partial y^2} + \frac{1}{4}\frac{\partial^2}{\partial z^2}\right]\right]M_x^B + 8(\Delta H_a)_x M = 0 . \tag{35}$$

Again, these reduce to simpler equations in the limit $\Delta H_A = 0$:

$$2M_y^A + \left[2 + a\sqrt{2}\frac{\partial}{\partial y} + a^2 \left[\frac{1}{2}\frac{\partial^2}{\partial y^2} + \frac{1}{4}\frac{\partial^2}{\partial z^2}\right]\right]M_y^B = 0 , \tag{36}$$

$$2M_x^A + \left[2 + a\sqrt{2}\frac{\partial}{\partial y} + a^2 \left[\frac{1}{2}\frac{\partial^2}{\partial y^2} + \frac{1}{4}\frac{\partial^2}{\partial z^2}\right]\right]M_x^B = 0 . \tag{37}$$

The remaining boundary condition comes from the requirement that the normal component of **B** and the tangential components of **H** are continuous. At the surfaces this gives

$$[(\pm Q_{||} + \alpha)\phi - 4\pi(\mathbf{M}_y^A + \mathbf{M}_y^B)] = 0 , \tag{38}$$

where the $+$ sign is appropriate for the upper surface of the film and the $-$ sign for the bottom surface. The remaining boundary conditions for the bottom of the film are obtained by replacing $+\partial/\partial y$ by $-\partial/\partial y$ in Eqs. (30)—(37).

The ten boundary conditions provide a set of ten homogeneous equations for the remaining unknowns $A^1 - A^{10}$. If we set the determinant of the coefficients equal to zero, this provides the condition which relates $Q_{||}$ to ω. The procedure outlined above is accomplished by a computer routine. To do this, one chooses a value for $Q_{||}$ and guesses a value for ω. Given these values, the program calculates the allowed values of α and the relationship between A_x and the other variables A_y, B_x, B_y, and ϕ^j. The program then computes the value of the determinant $D(Q_{||}, \omega)$ resulting from the boundary conditions. The problem is thus to find the values for which $D(Q_{||}, \omega)$ is zero. This search can be efficiently accomplished by a general root finding program, and one may then detail both the dispersion relation and the spatial variation of the various fields in the film.

C. (100) surface

The (100) surface differs considerably from the (110) surface in that the surface planes are made up of only one of the magnetic sublattices. This allows two distinct combinations of magnetic surfaces for the film. The same sublattice may occur at each boundary (symmetric combination), or a different sublattice may occur at each boundary (asymmetric combination). We will see that the spatial variation of the eigenmodes propagating in the film will be very sensitive to the combinations of magnetic surfaces.

Only one sublattice appears at each boundary, and as a result, the number of exchange boundary conditions is two per boundary. The magnetostatic boundary conditions provide a third equation for each boundary. Thus, only

six boundary condition equations are found. To have this be consistent with the equations of motion, only six of the ten α's may be used in superposing solutions. We can decide which α's to retain by noting that in the long-wavelength limit only the terms of $\alpha - \alpha^6$ will be significant when solving Eq. (13). We may then use Eqs. (19) and (20) in (18) to find the appropriate size alphas.

The procedure for finding the explicit boundary conditions is similar to that given in the preceding section, therefore we only state the results. For simplicity we have taken $\Delta H_a = 0$.

1. Symmetric surfaces

Here we find

$$4M_y^A + \left[4 \pm 2a\frac{\partial}{\partial y} + \frac{a^2}{2}\nabla^2\right]M_y^B = 0 , \tag{39}$$

$$4M_x^A + \left[4 \pm 2a\frac{\partial}{\partial y} + \frac{a^2}{2}\nabla^2\right]M_x^B = 0 . \tag{40}$$

The $+$ sign is appropriate for the upper surfaces, while the $-$ sign is for the lower surfaces.

2. Asymmetric surfaces

In this case,

$$4M_y^A + \left[4 + 2a\frac{\partial}{\partial y} + \frac{a^2}{2}\nabla^2\right]M_y^B = 0 , \tag{41}$$

$$4M_x^A + \left[4 + 2a\frac{\partial}{\partial y} + \frac{a^2}{2}\nabla^2\right]M_x^B = 0 . \tag{42}$$

The equations in the above two cases are appropriate for the upper surface. To obtain the equations for the lower surface, we replace $+\partial/\partial y$ by $-\partial/\partial y$ and replace M_k^A with M_k^B.

III. RESULTS

The thin-film dipole-exchange modes are a superposition of up to ten waves corresponding to the ten allowed solutions, $\alpha_1, \ldots, \alpha_{10}$, of the equation-of-motion matrix. The values of α are frequency dependent and may be real for some frequencies and imaginary for others. As a result, the final dipole-exchange mode has frequency-dependent bulk and surface characteristics. For a complete understanding of the dipole-exchange modes we examine the behavior of the five positive α's as a function of frequency in Fig. 2. The α's are plotted in dimensionless units as αa. These are solutions to Eq. (13) with $Q_{||}a = 0.01$ and propagation perpendicular to the z axis. The material parameters here and in the remainder of the paper are those appropriate for MnF$_2$ ($H_{ex} = 550$ kG, $H_a = 7.87$ kG, and $M = 0.6$ kG). One α is real for all fre-
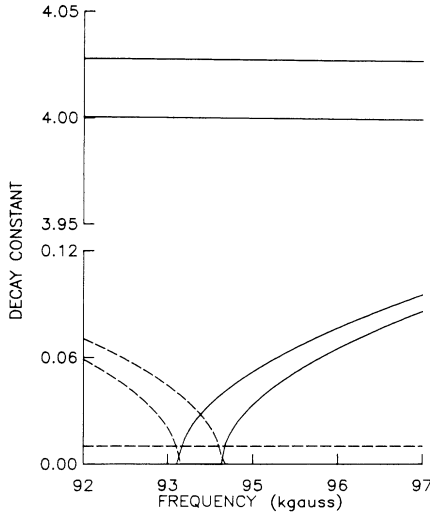
FIG. 2. Decay constants as functions of frequency for $Q_{||}a = 0.01$ and $\theta = 90°$. The solid lines are the imaginary part of the α's and represent bulk modes. The dashed lines are the real part of the α's and represent surface modes. Note how two of the α's change from real to imaginary as frequency increases.

quencies shown and has a nearly constant magnitude of approximately $Q_{||}$. This portion of the superposition comes from the dipolar fields and exists even in the long-

wavelength limit. The remaining values of α arise as one goes to shorter wavelengths. Two α's are real for frequencies below certain cutoff frequencies. The frequency at which they change from real to imaginary is different for each and depends on $Q_{||}$. For example, at $Q_{||}a = 0.0001$ one α becomes imaginary at 93 kG and the other becomes imaginary at 93.1 kG. At larger $Q_{||}a$, the two α's remain real until higher frequencies and change to imaginary at the same frequency. For $Q_{||}a = 0.1$, they both become imaginary at 97 kG.

The two largest α's are imaginary over the entire frequency range. They change very little with frequency and represent rapid spatial oscillations in the final superposition. These α's, however, have magnitudes greater than π/a and thus lie outside the first Brillouin zone. These do not represent physical solutions. We note, however, that similar results occur in the ferromagnetic case and are due to the inadequacy of the long-wavelength approximation. This feature does not generally invalidate our methods because in the superposition of waves the ones with these large values of α make only a very small contribution. Furthermore, these α's can be discarded when the boundary conditions do not require the full ten solutions.

Before proceeding to the exact solutions of the equation of motion matrix with the boundary conditions, it is useful to examine an interesting approximation which yields surprisingly good results. In the case of zero applied field, the determinant of Eq. (13) reduces to the simpler form obtained by Louden and Pincus:[15]

$$\omega/\gamma = \{H_a^2 + 2H_a + a^2 H_e (Q_{||}^2 + Q_y^2)[H_e + 4\pi M (Q_x^2 + Q_y^2)/(Q_{||}^2 + Q_y^2)]\}^{1/2} , \tag{43}$$

$$\omega/\gamma = \{H_a^2 + 2H_e[H_a + a^2 H_e (Q_{||}^2 + Q_y^2)]\}^{1/2} . \tag{44}$$

Here, terms to second order in $Q_{||}$ have been kept. To good approximation, we can calculate the frequency of the bulk modes by requiring Q_y to be an integral multiple of π/d; i.e., $Q_y = n\pi/d$. This simply says that the bulk modes are characterized by simple sinusoidal standing-wave patterns across the thickness of the film. When the full boundary conditions of Eqs. (32)—(37) or Eqs. (39)—(42) are applied, of course, they become more involved. Even so, the approximation is quite good and in Table I we present the frequencies obtained from the standing wave approximation. For comparison, we include frequencies obtained by the numerical solution of the equations of motion with the (110) surface and various boundary conditions. The two columns labeled "upper" and "lower" refer to bulk modes which originate from the upper or lower bulk bands in the case where only mean-field contributions are considered. We recall that for propagation perpendicular to the z axis, in the long-wavelength region there are two bulk bands whose frequencies are given by ω_1 and ω_2 (in the first section). In this limit there are an infinite number of bulk modes degenerate to each of these frequencies. When higher-order exchange energies are included, this degeneracy is removed and all the bulk modes are shifted up in frequency.

The resulting dispersion relations are given approximately by Eqs. (43) and (44). We are thus able to identify the upper-band bulk modes as obeying the dispersion (43) and the lower-band bulk modes as obeying (44). We note that

TABLE I. Frequencies from the (110) surface cases of free- and pinned-spin boundary conditions are compared to the results of the standing wave approximation. Here $Q_{||}a = 0.01$, $d/a = 300$, and $\theta = 90°$. The standing-wave approximation allows for the classification of modes according to their origin in the long-wavelength upper or lower bulk band limits.

| Standing Wave | | (110) Surface | |
Lower	Upper	Free	Pinned
		93.176	
		93.234	
93.460		93.470	93.528
93.593		93.601	93.673
93.814		93.816	93.843
	94.094	94.055	93.930
94.123		94.132	94.167
	94.228	94.199	94.194
94.519		94.426	94.429

the lower-band modes are completely free of dipolar energies in the very long-wavelength region and remain nearly free of dipolar energies even when exchange is included.

In the full boundary condition equations we saw that the boundary conditions contained a pinned-spin part and a free-spin part. In a real crystal, surface anisotropy fields differing from those in the bulk or different exchange constants at the surface may alter the importance of each term. It is therefore worthwhile to study the resulting dipole-exchange dispersions for each term separately. For both free and pinned examples, we use the (110) surface of MnF_2 as the film boundaries.

With the (110) surface at both film boundaries, there are boundary conditions on both M^A and M^B. For free spins, these boundary conditions are of the form $\partial M^A/\partial y = \partial M^B/\partial y = 0$, while for pinned spins we have $M^A = M^B = 0$ at the boundaries. The dispersion curves which follow are calculated for propagation perpendicular to the z axis ($\theta = 90°$), with $Q_{\parallel}a = 0.01$ and for zero applied field.

In Fig. 3, the dispersion curves for the free-spin boundary conditions are shown. The curves are plotted as frequency versus d/a, a dimensionless thickness. The most obvious feature is the removal of the bulk mode degeneracy and the increase in frequency from the very long-wavelength thick-film limit. As thickness increases, the bulk modes go toward the long-wavelength upper- and lower-bulk-band limits (ω_1 and ω_2). The lowest two curves are surface modes. Note how the surface modes curve down away from the bulk modes for small thicknesses. As will be seen when we study the potentials, one surface mode has even symmetry and the other has

odd symmetry. As thickness increases, the two surface modes become degenerate, reflecting the lack of coupling between the boundary surfaces.

As mentioned earlier, the surface modes are not strongly influenced by the inclusion of higher-order exchange terms or by variations in the thickness of the film. However, there is a small effect. We saw that the bulk modes were shifted up by effective fields which were proportional to the square of the wave vector. For surface modes the wave vector is complex, and the surface wave portions (the α's) lead to a decrease in the effective fields which leads to a small decrease in frequency. Indeed, the frequencies of the surface modes in Fig. 3 are about 0.5% lower than the values found when only mean field contributions are included.

Dispersion curves for pinned-spin boundary conditions are given in Fig. 4. Again, these are shown as frequency versus thickness. The most immediate difference between the pinned- and free-spin cases is that we find no predominately surface modes for the pinned case. While both the free- and pinned-spin frequencies are shifted away from the standing wave approximation, the pinned-spin frequencies see the largest shifts. From Table I, we see that there is an interesting pattern to the frequency shifts: the lower-band bulk modes are generally increased in frequency while the upper-band bulk modes are decreased in frequency.

Both the free- and pinned-spin dispersion curves display the feature of mode repulsion and crossing. Some bulk modes cross without interaction while others repel. As will be shown below, the modes which repel have the same symmetry while the modes which cross have oppo-
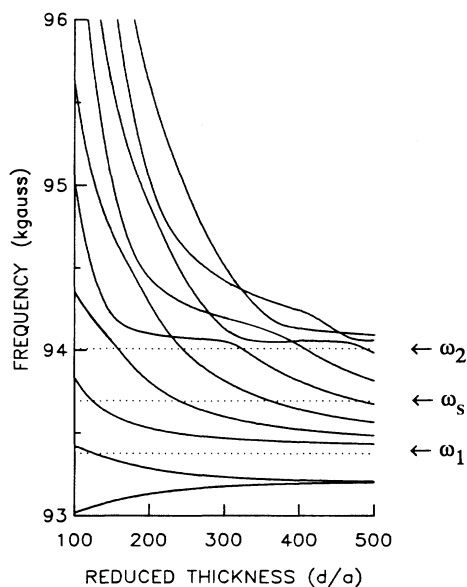

FIG. 3. Frequency as a function of number of layers, d/a, for the (110) surface at the film boundaries. There is no surface pinning. There is no applied field, $Q_{\parallel}a = 0.01$ and $\theta = 90°$. The two lowest curves are surface modes and the higher curves are the first few bulk modes. Note how some bulk modes cross without interaction while others repel.
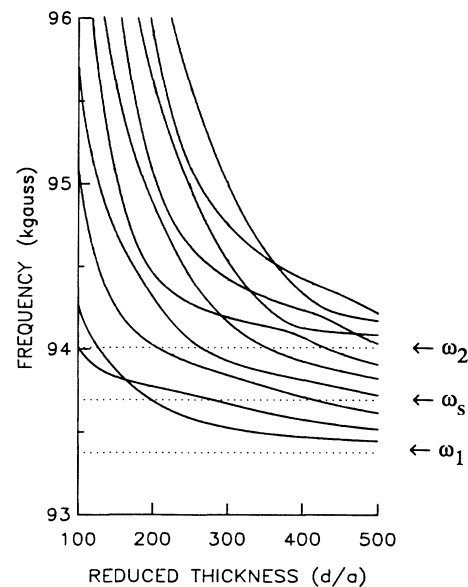
FIG. 4. Frequency as a function of number of layers, d/a, for the (110) surface at the film boundaries. The spins are completely pinned at the surface. There is no applied field, $Q_{\parallel}a = 0.01$ and $\theta = 90°$. The frequencies are shifted from the free-spin case according to whether a mode belongs to the upper or lower long-wavelength bulk band.

site symmetry.

To understand the features displayed in the dispersion curves, such as the mode crossings and repulsions, we must investigate the mode symmetries. In the long-wavelength region, or for very thick films, the allowed modes always display even or odd symmetry about the midplane of the film *except* in the presence of an applied field. This is not the case for very thin films, however, where the symmetry of the dipole-exchange modes depends on the film's microscopic surface structure. To show this, we first investigate the case where the (110)

surface appears at both film boundaries, and later we discuss the various possibilities for the (100) surface.

In discussing the symmetry properties of the dipole-exchange modes, it is useful to consider the spin-spin correlation function $M_{ij}(\mathbf{x},\mathbf{x}';t,t')$ defined as

$$M_{ij}(\mathbf{x},\mathbf{x}';t,t') = \langle M_i(\mathbf{x},t)M_j(\mathbf{x}',t') \rangle \ . \tag{45}$$

The subscripts here identify the spatial component of the magnetization. Since the crystal has translational invariance parallel to the surface, we may write $M_{ij}(\mathbf{x},\mathbf{x}';t,t')$ in terms of its Fourier transform as

$$M_{ij}(\mathbf{x},\mathbf{x}';t,t') = \frac{1}{(2\pi)^3} \int d\mathbf{Q}_{||}d\omega M_{ij}(\mathbf{Q}_{||},\omega,y,y')\exp[i\mathbf{Q}_{||}\cdot(\mathbf{x}_{||} - \mathbf{x}'_{||}) - i\omega(t - t')] \ . \tag{46}$$

Here $\mathbf{x}_{||}$ is the projection of $\mathbf{x}$ on the plane parallel to the surface. The diagonal element $M_{xx}(\mathbf{Q}_{||},\omega,y,y)dy$, for example, is interpreted as measuring the probability of finding a spin fluctuation in the x direction with wave vector $\mathbf{Q}_{||}$ and frequency ω, in a slab of thickness dy a distance y from the surface. The time-averaged values of the square of the magnetizations given in Eqs. (21)—(24) can also be interpreted as probabilities dependent on Y, and can thus be related to the diagonal correlation function elements.

Suppose the (110) surface is parallel to the film surfaces. The A and B sublattice magnetizations are written $\mathbf{M}^A(\mathbf{x}_{||},y)$ and $\mathbf{M}^B(\mathbf{x}_{||},y)$. A symmetry operation for this configuration is a reflection through the midplane, followed by a translation along the x axis by the lattice constant a. By investigating the effects of these operations on the correlation function $M_{xx}(\mathbf{Q}_{||},\omega,y)$ we can discover the allowed symmetries for the fluctuating portions of the magnetization.

Reflection through the midplane changes $M_x^A(x,y,z)$ to $-M_x^B(x,-y,z)$, since a spin reverses under reflection changing both the sign of the x component and the direction of the z component. Translation in the x direction by a returns the lattice to its original configuration. Under these operations, the correlation function $M_{xx}^A(\mathbf{x}_{||},\mathbf{x}_{||};y,y')$ becomes $M_{xx}^B(\mathbf{x}_{||}+a\mathbf{x},\mathbf{x}_{||}+a\mathbf{x};-y,-y')$. Since we have performed a symmetry operation, the correlation functions must be equal. Writing these in their Fourier expansions and equating coefficients, we have

$$M_{xx}^A(\mathbf{Q}_{||},\omega;y) = M_{xx}^B(\mathbf{Q}_{||},\omega,-y) \ . \tag{47}$$

The translation along $\mathbf{x}$ by a has no effect on the integral of Eqs. (46) since both $\mathbf{x}_{||}$ and $\mathbf{x}'_{||}$ are translated equal distances.

We can now see that while the magnetization of any one sublattice need not be symmetrical about the midplane, the sum of both sublattice magnetizations is. Using Eq. (47), we find

$$M_{xx}^A(\mathbf{Q}_{||},\omega,y) + M_{xx}^B(\mathbf{Q}_{||},\omega,y) = M_{xx}^B(\mathbf{Q}_{||},\omega,-y)$$
$$+ M_{xx}^A(\mathbf{Q}_{||},\omega,-y) \ . \tag{48}$$

A similar argument may be made for the diagonal element $M_{yy}(\mathbf{Q}_{||},\omega,y)$. We obtain

$$M_{yy}^A(\mathbf{Q}_{||},\omega,y) + M_{yy}^B(\mathbf{Q}_{||},\omega,y) = M_{yy}^B(\mathbf{Q}_{||},\omega,-y)$$
$$+ M_{yy}^A(\mathbf{Q}_{||},\omega,-y) \ . \tag{49}$$

The preceding argument shows that if we time average the square of M_x^A and add the time average of the square of M_x^B, we obtain a function which is even about the midplane. One can now easily show that if we first add M_x^A and M_x^B and then square and time average, this result is also symmetric about the midplane. In fact, it is this latter quantity that we will display in our figures. The quantity A_x plotted in our figures is thus given by $A_x = [\langle (M_x^A + M_x^B)^2 \rangle]^{1/2}$. Similarly, $A_y = [\langle (M_y^A + M_y^B)^2 \rangle]^{1/2}$.

We now wish to emphasize an important point. The preceding symmetry operations are valid for a finite thin film if the (110) surface is present at both film boundaries but these operations do not necessarily hold when other surfaces are present at the boundaries. As we shall see, this can lead to interesting localization effects for those cases where the symmetry operations of a reflection about the midplane followed by a translation parallel to the midplane do not hold.

The symmetries of the dipole-exchange modes can be displayed by plotting the time average of the square of the magnetizations and dipolar potentials as a function of y, the coordinate normal to the film surfaces. In Fig. 5 we
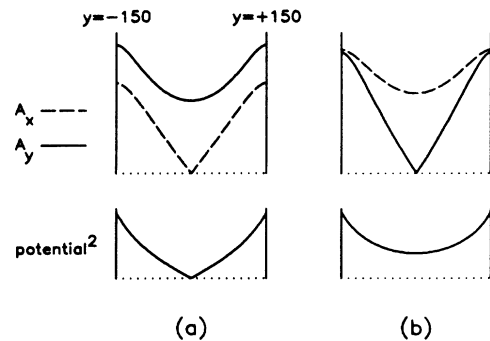

FIG. 5. Magnitude of the potentials and magnetizations as a function of depth, y, for the case of (110) surfaces. There is no surface pinning. The two sets are for the surface modes of Fig. 4 with $d/a = 300$. The lowest frequency surface mode is shown in (a) and the highest surface mode is shown in (b).

present these results for the surface modes for free-spin boundary conditions on a (110) surface. The reduced thickness is $d/a = 300$, the wave vector is given by $Q_\| d = 3.0$, and the propagation angle is $\theta = 90°$. From the dipolar potentials, these are clearly surface modes exponentially decaying from each surface. The lowest frequency mode has odd symmetry about the midplane, and the other surface mode has even symmetry about the midplane. We note that since we have plotted the time average of the square of the fluctuation, the curves in Fig. 5 and below are always positive and even. However, it is relatively easy to determine the symmetry (odd or even) of the modes. For example, modes which do not go to zero at the midplane must be even.

If these results are compared to those found in thicker films where the only exchange contribution comes from the mean field, one finds that the lower frequency surface mode is even about the midplane. This is in contrast to the above result. To see that our new results are consistent, we have extended our calculations to much smaller wave vectors and we find that the modes do indeed cross.

The magnetizations in Fig. 5 have their greatest magnitude at the surface, as in a surface mode, but the curvature of the magnetizations suggests the standing-wave character of a bulk mode. There is an interesting pattern to the symmetries of the magnetizations. In the lowest frequency mode, the x component of the magnetization has odd symmetry, while the y component is even. In the

next highest mode, the situation is reversed, with the x component now having even symmetry and the y component having odd symmetry. We note that the two surface modes have opposite symmetry in all respects (the dipolar potential, and the x and y components of magnetization) which allows them to have the same energy in certain circumstances. At large thicknesses the two surface modes merge together.

The first four bulk modes for the free-spin conditions above are shown in Fig. 6. We note that the distinction between surface and bulk modes is somewhat artificial here. The magnetizations and potentials in Fig. 6 both look somewhat like sinusoidal standing waves across the thickness of the film, and hence we call them bulk modes. We do see some influence of the real α's in the superposition, creating surface-wave-like variations in the magnetizations and potentials.

The x and y components of the bulk modes magnetizations exhibit the same kind of symmetry reversal as seen in the surface modes. The symmetries of the bulk modes of Figs. 6(c) and 6(d) are opposite in all respects while the modes of Fig. 6(b) have the same symmetry as that of Fig. 6(d). Referring to the dispersion curves of Fig. 3, we see that the same symmetry modes [Figs. 6(b) and 6(d)] repel, while the opposite symmetry modes [Figs. 6(c) and 6(d)] cross without interaction.

The potentials and magnetizations for pinned spin boundary conditions are shown in Fig. 7. The wave vector is again $Q_\| d = 3.0$, $\theta = 90°$, and $d/a = 300$. There is
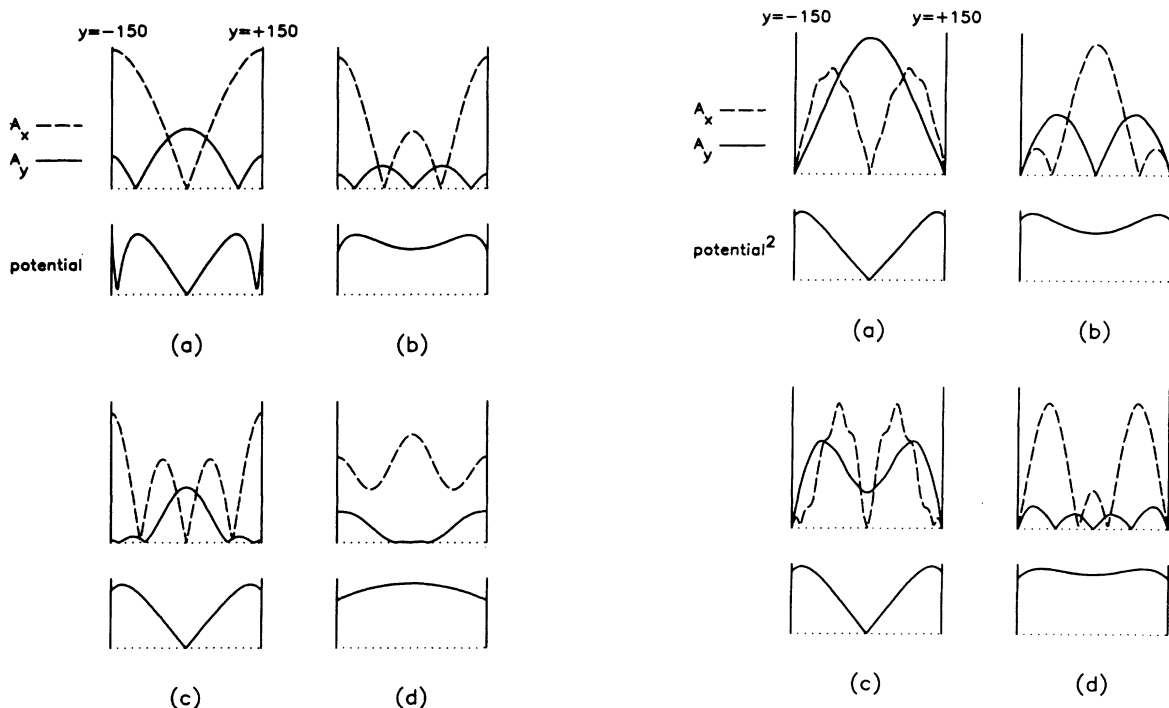

FIG. 6. Magnitude of the potentials and magnetizations as a function of y for the case of (110) surfaces. There is no surface pinning. The four lowest frequency bulk modes from Fig. 4 are represented with (a) having the lowest frequency and (d) the highest.

FIG. 7. Magnitude of the potentials and magnetizations as functions of y for the (110) surface at the boundaries. The spins are fully pinned at the surfaces. Here the four lowest frequency modes of Fig. 5 are presented at $d/a = 300$. Again note the alternating symmetries of the potentials and magnetization components.

no applied field. Here we present the four lowest frequency modes of the pinned spin dispersion of Fig. 4. The components of the magnetization show the same symmetry reversal as in the free-spin case, and the bulk modes cross and repel exactly as before.

We have calculated the dispersion relations when both the free-spin and the pinned-spin terms appear in the complete boundary conditions. The results are unfortunately not correct. When the full boundary conditions are used, the unphysical, large α partial waves are strongly represented in the superposition of the partial waves.

Up to now we have discussed only symmetrical films; that is, films which have symmetry operations which take them into themselves. We now consider films where the (100) surface is parallel to the film boundaries. If sublattice A appears at one boundary, and sublattice B appears at the other boundary, the film will be taken into itself by the simple symmetry operation of reflection about the midplane, and the time average of $(\mathbf{M}^A+\mathbf{M}^B)^2$ will again be symmetrical about the midplane. Should the same sublattice appear at both boundaries, the correlations functions $M_{xx}(\mathbf{Q}_{||},\omega,y)$ or $M_{yy}(\mathbf{Q}_{||},\omega,y)$ can no longer be related to the equivalent correlation functions involving $\mathbf{Q}_{||}$, and $-y$. Under *any* symmetry operation which takes $+y$ to $-y$, the x component of the wave vector is also changed from Q_x to $-Q_x$. As a result, for a wave with a fixed $\mathbf{Q}_{||}$, there is no requirement that the magnetizations be symmetric about the midplane. This is clearly seen by the profiles of the magnetizations and potentials, which we will discuss shortly. It is also reflected by the dispersion curves for the two boundary cases.

We note that for the asymmetrical boundary film, the propagation is nonreciprocal, i.e., $\omega(Q_{||})\neq\omega(-Q_{||})$. Al-

TABLE II. Frequencies from the (100) surface cases of symmetrical and asymmetrical boundaries are compared. The asymmetrical boundary film frequencies are tabulated for the case of no applied field and the case of $H_0=0.1$ kG. All frequencies are for the parameters $d/a=300$, $Q_{||}a=0.01$, and $\theta=90°$.

Symmetric $(H_0=0)$	Asymmetric $(H_0=0)$	Asymmetric $(H_0=0.1)$
93.528	93.519	93.500
93.678	93.658	93.637
93.850	93.840	93.828
93.923	93.967	93.978
94.162	94.192	94.188
94.204	94.204	94.215
94.421	94.439	94.451
94.548	94.550	94.543

though this effect can be significant, we do not pursue this topic here, but it is planned to be discussed in a subsequent paper.[21] A similar effect has been found for superlattices composed of ferromagnetic films which alternate in magnetic direction.[22]

The dispersion curves and profiles for the (100) surface when sublattice A is at $y=+d/2$ and sublattice B is at $y=-d/2$ are nearly identical with those presented earlier for the pinned case of the (110) surface. Although the complete boundary conditions are used, it is clear that the pinning terms dominate in this case.
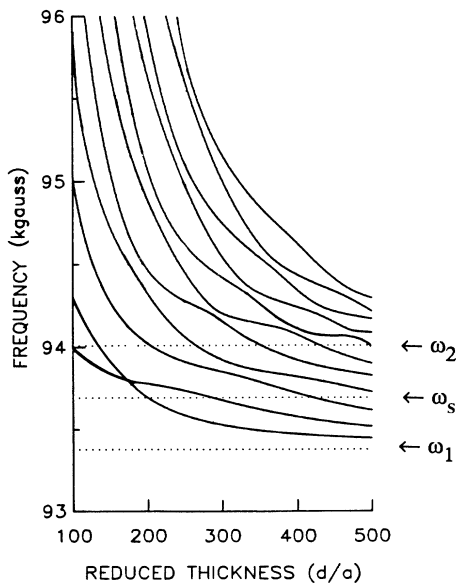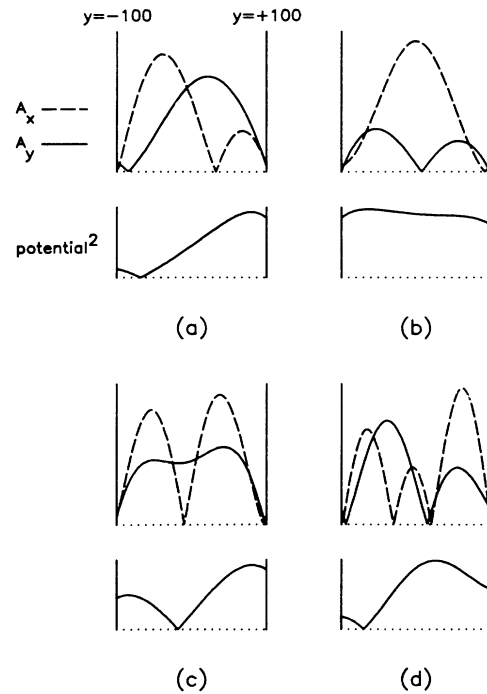

FIG. 8. Frequency as a function of number of layers for the (100) surface at the film boundaries. The A sublattice appears at both film boundaries. There is no applied field, $Q_{||}a=0.01$, and $\theta=90°$. The frequencies are shifted significantly from the case where different sublattices appear at each boundary (Fig. 8).

FIG. 9. Magnitude of the potentials and magnetizations as a function of y for the (100) surface at both boundaries. Sublattice A appears at both film boundaries. The four lowest frequency modes of Fig. 8 are profiled at $d/a=200$. Note how the potentials and magnetizations are localized at the surfaces even though there is no applied field.

The dispersion curves for the (100) surface with sublattice A at both boundaries are given in Fig. 8. There is no applied field. Here we find that the frequencies are significantly different from the previous considered case. There are no crossings in the dispersion curve, only repulsions. A comparison of the frequencies for the different surfaces is given in Table II.

The difference between the two (100) surface film configurations is even more striking when we compare the potentials and magnetizations for each case. The potentials and magnetizations for the four lowest frequency modes for the films with asymmetric boundaries are nearly identical to those in Fig. 7. The same four modes for the symmetric boundary film are shown in Fig. 9. In comparing these two figures, one comes to a conclusion that the asymmetrical boundary film has modes which are symmetric about the midplane, but the symmetrical boundary film has modes which are asymmetric about the midplane. This result is consistent with our earlier symmetry argument. Since the modes for the same-surface film no longer have odd or even symmetry about the midplane, there is no way for two modes to have completely opposite symmetry. This explains why only repulsions are seen in the dispersion curves in Fig. 8.

The modes for the film with the symmetric surfaces can be quite localized. The localization is similar to what would happen for the asymmetrical boundary film if it

were subject to a small applied field. This is, in fact, one way of viewing the symmetrical boundary film. For the same sublattice to appear at both boundaries, there must be an odd number of sublattice layers. This means there is a net magnetization in the film due to one extra sublattice layer. We note that in recent work by Hinchey and Mills,[23] the number of layers (even or odd) plays an important role in superlattices with antiferromagnets.

We explore this idea further in Fig. 10 where the first four modes of the asymmetrical film are profiled with the same parameters as in Fig. 9, but now with an applied field of 0.1 kG. The localization seen in Fig. 10 is very similar to the results for the symmetrical boundary film seen in Fig. 9. A comparison of the frequencies is presented in Table II.

Under this interpretation, we would expect that the localization of modes in a symmetrical boundary film should decrease for larger thicknesses where the surfaces might have less of an influence. This is indeed the case as is seen in Fig. 11. In this figure we profile the first four modes for a like boundary film with a thickness of $d/a = 600$ and $Q_{\parallel}d = 6$. We see that there is still a noticeable localization, but it is much less pronounced than in the preceding figures.

In the dispersion curves previously considered, we have varied the film thickness while holding the wavelength constant. In Fig. 12 we hold the thickness constant, at
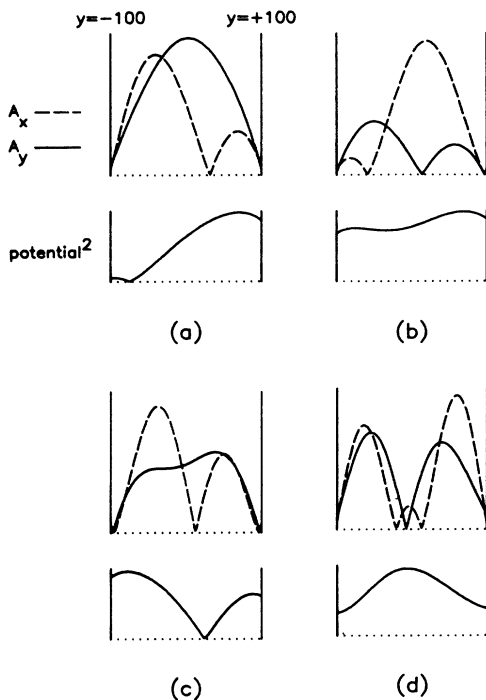

FIG. 10. Magnitude of the potentials and magnetizations as a function of y for the (100) surface at both boundaries. Sublattice A appears at $y = d/2$ and sublattice B appears at $y = -d/2$. Here we include an applied field of magnitude 0.1 kG. The lowest four bulk modes are profiled at $d/a = 200$. We see that the presence of an applied field localizes the modes to one or the other boundary.
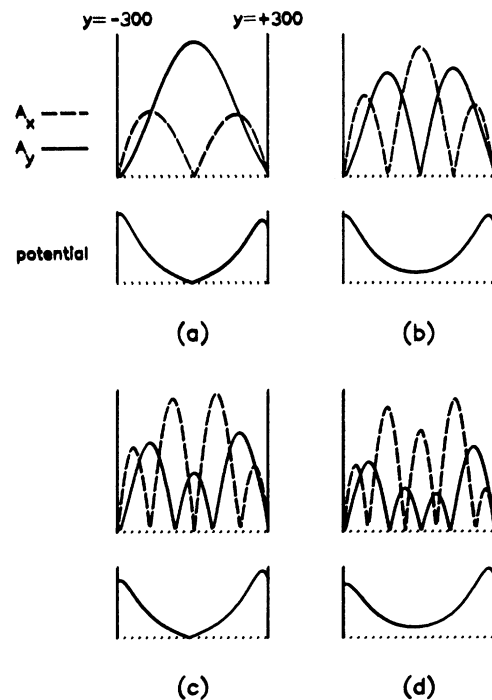

FIG. 11. Magnitude of the potentials and magnetizations as a function of y for the (100) surface at both boundaries but with sublattice A at both $y = d/2$ and $y = -d/2$. The reduced thickness is 600 and there is no applied field. We see that the modes are much less localized than the thinner film case of Fig. 9.
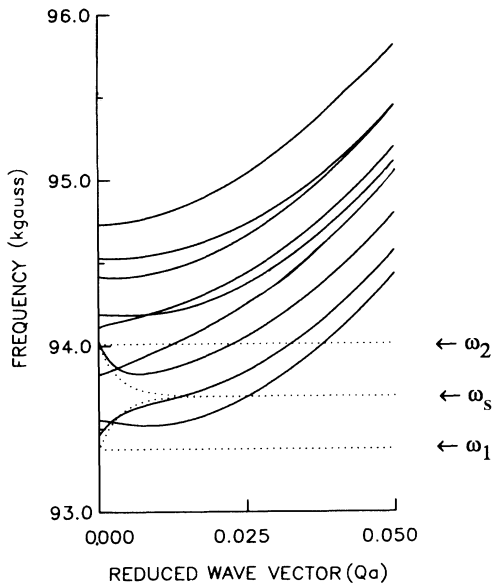
FIG. 12. Frequency as a function of reduced wave vector $Q_{\parallel}a$ for the (100) surface at both boundaries. Sublattice A appears at $y = d/2$ and sublattice B appears at $y = -d/2$. There is no applied field, $\theta = 90°$, and $d/a = 300$. As $Q_{\parallel}a$ goes toward zero, two modes approach the long-wavelength surface mode limit.

$d/a = 300$, and vary the wavelength. As the wavelength decreases, the mode frequencies increase with increasing Q. Crossings of opposite symmetry modes occur as before. We note that two modes approach the long-wavelength surface mode limit (shown by the dotted lines for ω_s) as Qa goes to zero.

Finally, we explore the effect of dynamic pinning introduced earlier. In the derivation of the boundary conditions in Sec. II, we saw that under certain circumstances the pinned terms could cancel leaving only the free-spin terms. In the limit $Q_x \ll Q_y$, this would occur for the x components of the magnetizations in the upper-band bulk
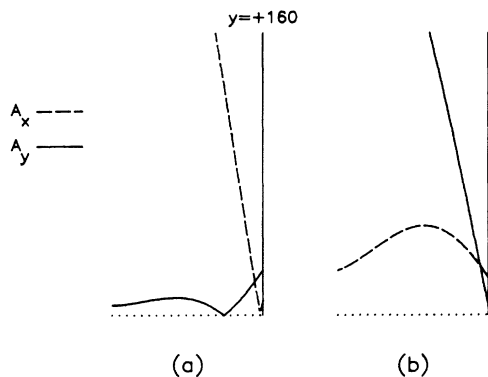

FIG. 13. Behavior of the magnetizations at the boundaries. The two modes are profiled for the (100) surface asymmetrical boundary film with $D/a = 320$ and $Q_{\parallel}a = 0.01$. The mode in (a) is at frequency 94.14 kG and belongs to the lower bulk band set. The mode in (b) is at 94.17 kG and belongs to the upper bulk band set. The x component is pinned in (a) while the y component is pinned in (b).

modes and for the y components of the lower bulk band magnetizations. The y components of the upper bulk band magnetizations would still feel the pinned-spin terms as would the x components in the lower bulk band modes.

We see this effect in the profile of the magnetizations shown in Fig. 13. These are plotted for the fifth and sixth highest modes in frequency. The reduced thickness is $d/a = 320$. In Fig. 13(a) a bulk mode from the lower bulk band set shows a pinned x component of magnetization while the y component seems to obey a combination of pinned and free boundary conditions. In Fig. 13(b), the mode belongs to the upper-band set, and the y component of the magnetization is fully pinned while the x component shows only some pinning.

IV. SUMMARY

In this paper we have considered the problem of spin waves in thin antiferromagnetic films. We find that to properly describe the excitations, both dipolar and exchange contributions must be included. We have derived boundary conditions appropriate to several possible film surface structures. Seeking solutions to the equations of motion which are consistent with these boundary conditions, we have found fundamental and sometimes complicated relations between the properties of the dipole-exchange modes and the film's magnetic surface structure. Our major results can be summarized as follows:

(1) As the thickness is reduced, the surface modes decrease slightly in frequency, while the bulk modes show a significant increase in frequency. For propagation perpendicular to the easy axis, the frequencies of the bulk modes are approximated reasonably well by assuming that the mode profiles perpendicular to the film surfaces are simple standing waves with wave vectors given by $Q_y = n\pi/d$ and by using Eqs. (43) and (44).

(2) The spin-wave frequencies depend on the relative magnitudes of the free- and pinned-spin terms in the boundary conditions. Modes which come from the lower bulk band in the long-wavelength limit have frequencies which increase with surface pinning. Upper bulk band modes decrease in frequency with surface pinning.

(3) The pinned spin terms in the boundary conditions can cancel in certain limits, leaving one component of the magnetizations essentially unpinned.

(4) In the dispersion curves, we see both mode repulsion and mode crossings. When we examine the profiles of the magnetizations and the dipolar potential, we see that the modes which cross have opposite symmetry in all respects. Similarly, the modes which repel have the same symmetry.

(5) When the film has surfaces such that there exist symmetry operations which can change y to $-y$ but leave the wave vector Q_x unchanged, the spin wave will have even or odd symmetry about the midplane. This will occur for the (110) surfaces and will also occur for the (100) surface if the top layer is from a different sublattice than the bottom layer.

(6) If the film has surfaces such that there do not exist symmetry operations which take y to $-y$ and leave Q_x unchanged the spin wave will be somewhat localized to one surface of the film. Surface modes will be strongly

localized, and bulk modes will exhibit weaking localization. The effect is analogous to the application of a small magnetic field along the easy axis. This situation will occur for a film with (100) surfaces where spins from one sublattice only appear at both surfaces.

[1]J. C. Sethares, J. Appl. Phys. 53, 2646 (1983).

[2]M. S. Sodha and N. C. Srivastava, *Microwave Propagation in Ferrimagnetics* (Plenum, New York, 1981).

[3]R. L. Stamps and R. E. Camley, J. Appl. Phys. 56, 3497 (1984).

[4]R. E. Camley, Phys. Rev. Lett. 45, 283 (1980).

[5]B. Luthi, D. L. Mills, and R. E. Camley, Phys. Rev. B 28, 1475 (1983).

[6]V. V. Tarasenko, and V. D. Kharitonov, Zh. Eksp. Teor. Fiz. 60, 2321 (1971) [Sov. Phys.—JETP 33, 1246 (1971)].

[7]L. Remer, B. Luthi, H. Sauer, R. Geick, and R. E. Camley, Phys. Rev. Lett. 56, 2752 (1986).

[8]G. T. Rado and J. R. Weertman, J. Phys. Chem. Solids 11, 315 (1959).

[9]J. T. Yu, R. A. Turk, and P. E. Wigen, Phys. Rev. B 11, 420 (1975).

[10]R. Henry, S. D. Brown, P. E. Wigen, and P. J. Besser, Phys. Rev. Lett. 28, 1272 (1972).

[11]R. E. Camley, T. S. Rahman, and D. L. Mills, Phys. Rev. B 23, 1226 (1981).

[12]R. E. Camley and D. L. Mills, Phys. Rev. B 18, 4821 (1978).

[13]R. E. Camley, P. Grunberg, and C. M. Mayr, Phys. Rev. B 26, 2609 (1982).

[14]M. Lui, J. Drucker, A. R. King, J. P. Kotthaus, P. K. Hansma, and V. Jaccarino, Phys. Rev. B 33, 7720 (1986).

[15]R. Louden and P. Pincus, Phys. Rev. 132, 673 (1963).

[16]T. Wolfram and R. E. Dewames, Prog. Surf. Sci. 2, 233 (1972).

[17]M. Sparks, J. Appl. Phys. 11, 1018 (1970).

[18]This can be shown by solving the long-wavelength equations of motion for the normal modes. For the lower frequency solution, one finds $k_x(M_x + M_x) + k_y(M_y + M_y) = 0$. For the higher frequency solution, $k_x(M_y + M_y) - k_y(M_x + M_x) = 0$.

[19]F. Hoffmann, Phys. Status Solidi 41, 807 (1970).

[20]M. Sparks, Phys. Rev. B 1, 3831 (1970).

[21]R. L. Stamps and R. E. Camley (unpublished).

[22]K. Mika and P. Grünberg, Phys. Rev. B 31, 4465 (1985).

[23]L. Hinchey and D. L. Mills, J. Appl. Phys. 57, 3687 (1985) and J. Magn. Magn. Mater. 54—57, 805 (1986); Phys. Rev. B 33, 3329 (1986).